OPTIMAL DESIGN OF SINGLE PHASE DUAL ACTIVE BRIDGE CONVERTER FOR FAST EV CHARGING USING MULTI SINE COSINE ALGORITHM

Rajendra K1*, Rambabu Ch2, Sathishkumar R3 and Lakshminarasimman L4

- ^{1.} Research Scholar, Annamalai University, Annamalai Nagar 608002, India.
- ^{2.} Professor, Department of EEE, Sri Vasavi Engineering College(A), Tadepalligudem, Andhra Pradesh, India.
- ^{3.} Associate Professor, Department of Electrical and Electronics Engineering, SRM TRP Engineering College, Tiruchirappalli, Tamilnadu, India.
- ⁴ Professor. Department of Electrical Engineering, Annamalai University, Annamalai Nagar 608002, India.

ABSTRACT

The Dual Active Bridge (DAB) converter is a bidirectional isolated DC-DC topology widely adopted in medium and high-power applications such as electric vehicle fast charging, renewable integration, and energy storage systems. When interfaced with the utility grid through inverters or directly coupled to AC systems, the switching dynamics of the DAB introduce unique stability and power quality challenges. DAB converters inherently produce AC waveforms between their H-bridges, resulting in significant harmonic content due to switching actions and modulation schemes. This paper discusses Sine Ware Correlation (SWC), an efficient methodology in the estimation of interharmonics. This paper also explores the implementation of Multi Since Cosine Algorithm (MSCA) based methodology for optimal selection of DAB parameters and tuning the current regulator in order to minimize the amplitude of interharmonics.

Keywords: DAB, EV Fast Charging, Interharmonics, MSCA, SWC.

1. INTRODUCTION

In both industrialized and developing nations, the transportation sector is a significant source of greenhouse gas (GHG) emissions in addition to fossil fuel-based power plants. The most recent advancement in vehicle technology is going toward electric cars (EVs) with electric motors and battery storage to reduce GHG emissions from the transportation sector. The combination of environmental concerns, technological advancements, cost savings, and supportive policies has created a strong motivation for the increased adoption of electric vehicles.

As the adoption of electric vehicles continues to grow, there is an increasing focus on expanding and improving the fast-charging infrastructure to make electric vehicles more viable. For a better recharging experience for the EV drivers, the recharging time of EV at FCSs needs to be comparable to the refuelling time of ICEVs. Hence, the power of FC keeps increasing in the past years. To distinguish with FC (rated at 50 kW), the state of art multi-hundred-kilowatt charging is named ultra-fast charging (UFC), which is gaining more attention in recent years.

The tremendously growing EV population, will replace fuel stations by fast-charging stations soon. This will draw a significant amount of power from the electricity grid, especially when multiple vehicles are charging simultaneously. This increased demand can create PQ issues. These issues at the point of common coupling can be broadly classified as voltage fluctuation, harmonic stability, and harmonic emission. These issues can also have significant adverse effects on electrical equipment and interference with control and protection signals in power supply lines. This will result in significant energy losses and challenges to the system's stability. As a result, it is critical to analyse and develop proper mitigation approaches thereby increasing fast charging efficiency.

A battery charger must be efficient and reliable, with high power density, low cost, and low volume and weight. Its operation depends on components, control, and switching strategies. An EV charger must ensure that the utility current is drawn with low distortion to minimize power quality impact and at high power factor to maximize the real power available from a utility outlet. With the topologies allowing bi-directional energy flow, the vehicle-togrid (V2G) function is developed to not only minimize the grid impacts of EV charging but also provide grid support, e.g. load balancing, frequency and voltage regulation.

1.1 Dual Active Bridge (DAB) Converters for Fast EV Charging

A Dual Active Bridge (DAB) converter is a bidirectional isolated DC–DC converter. It connects two DC systems through a high-frequency transformer, allowing power transfer in both directions. Figure 1 shows the schematic of a single-phase DAB. The major components of the bidirectional Dual Active Bridge-based EV battery charging system design are a bidirectional DC/AC converter, followed by a high-frequency transformer feeding a bidirectional AC/DC converter, which in turn charges the EV battery. The transformer provides galvanic isolation and voltage scaling. The DAB operates by transferring power through phase shift control between the two bridges.(Veerakgoundar & Subramaniam, 2025)

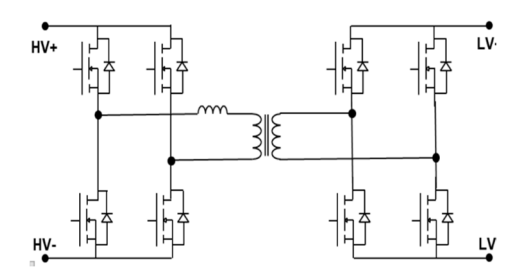


Fig. 1 Dual Active Bridge Converter

The Dual Active Bridge topology leverages high-performance MOSFETs, often made of SiC (Silicon Carbide), to handle high voltages and rapid switching needed for EV fast charging. The DAB provides galvanic isolation via a high-frequency transformer and enables bidirectional power flow, allowing vehicle-to-grid (V2G) applications and flexible energy management. (Gill et al., 2019)

Typical MOSFET-based DAB fast charger features a two-stage topology. The first stage is an active front end (AFE) converting AC grid input to high-voltage DC. The second is the DAB, which regulates charging and provides isolation, with modular designs scaling output power up to 300 kW.(Liang et al., 2019)

The DAB uses phase-shift modulation for bidirectional DC-DC conversion with zero-voltage switching (ZVS), minimizing switching losses and improving thermal management. SiC MOSFETs further enhance efficiency due to their fast switching and low recovery charge.

1.2 Grid Disturbances due to DAB

While DABs bidirectional power flow and galvanic isolation make it attractive, when tied to the AC grid, new challenges arise most notably sub-synchronous, interharmonic and harmonic distortion. The core of the issue lies in the control and interaction of these power-electronic interfaces with the traditional AC grid. The grid was designed for large, synchronous generators that provide inherent inertia (resistance to frequency changes) and natural fault current. DABs and other inverters behave very differently.

The primary mechanisms for causing disturbances are loss of Synchronization, fault-induced delayed voltage recovery (FIDVR), sub-synchronous oscillations (SSO) and harmonic distortion, lack of inertia, etc. Grid disturbances due to DABs are not a flaw in the DAB topology itself but a challenge of integrating large numbers of fast-acting, inertia-less power electronic devices into a grid designed for slow-acting synchronous machines.

The core issues are loss of synchronization, poor voltage recovery, and unwanted oscillations. Solving this requires a combination of better hardware standards, smarter software controls (especially grid-forming inverters), and updated grid planning practices.

The high-frequency switching (in the kHz range) of DAB converters can interact with grid impedances (lines, transformers, capacitors) to create resonances. These resonances can manifest as currents and voltages oscillating at frequencies below the fundamental 50/60 Hz (sub-synchronous) or as integer multiples of the fundamental frequency (harmonics, e.g., 150Hz, 250Hz). These oscillations can overheat and damage rotating machinery (generators, motors) by causing torsional stress, distort the voltage waveform affecting the performance of other sensitive equipment and nuisance tripping of protection relays.

The study of grid disturbances caused by high-power electronic converters such as the Dual Active Bridge (DAB) has gained significant traction in recent years, particularly in the context of fast charging of electric vehicles (EVs). Early work by Qin et al. provided a rigorous modelling framework for DAB converters under wide load ranges, highlighting how modulation schemes and transformer parasitics affect harmonic distortion and switching behaviour. This foundational work established that while DABs are attractive for bidirectional, isolated, high-power conversion, their nonlinear dynamics can excite both harmonic and interharmonic components under non-ideal conditions.

Building on this, Ataullah et al. conducted a comprehensive comparative study of DAB topologies, including high-frequency transformers and control strategies. Their results, validated with experimental prototypes, showed that while conventional harmonics (THD around 1.5–1.7%) could be kept within IEEE-519 limits, the high-frequency spectral content induced by leakage inductances and parasitics could not be ignored. This pointed toward the need to investigate harmonic and interharmonic ranges, especially for fast-charging use cases where multiple converters are deployed in parallel.

From a system-level perspective, Cinik et al. optimized efficiency and cost trade-offs for 350 kW modular fast chargers based on seven 50 kW DAB modules. Their findings emphasize the role of switching frequency selection (≈30 kHz) not only in efficiency but also in determining the magnitude and distribution of high-frequency emissions. As switching frequency directly governs the supraharmonic spectrum (2–150 kHz), this study underscores the link between economic design choices and power quality.

The standards landscape is also important. IEEE 519 and IEC 61000-4-7 provide guidelines for harmonic and interharmonic limits, but they primarily address frequencies up to 2 kHz. For India, the CEA standards outline harmonic limits for distributed generation and EV chargers, but do not explicitly regulate supraharmonics. This regulatory gap is particularly concerning for large-scale DAB deployment in Indian distribution networks, where weak grids and resonance with compensation devices can amplify emissions.

More recent studies have shifted toward supraharmonic and transient analysis. Rajkumar et al. compared supraharmonic emissions from different DC fast charger converter topologies. Their work demonstrated that switching frequency, modulation strategy, and load profile significantly influence the 2–150 kHz band, confirming that DAB converters, if not carefully controlled, can inject measurable supraharmonic currents into the grid.

At the harmonic level, Pan et al., investigated second harmonic current reduction in DABs using an impedance perspective. Their study revealed that impedance mismatches between the converter and the grid amplify low-order harmonics, particularly under Dual Phase Shift (DPS) control. This directly connects converter design to classical sub-synchronous and harmonic oscillations in the grid, illustrating how certain modulation schemes may worsen distortion.

Expanding further, Joarder et al., provided a detailed framework for harmonic modelling and control of DAB converters in microgrids. They proposed analytical models that predict harmonic spectra based on converter parameters, making it possible to design more effective control strategies and filters. Such work bridges the gap between theoretical harmonic analysis and practical microgrid deployment.

Beyond conventional harmonics, the impact of supraharmonics on power networks has been documented by Mariscotti et al., who showed how 2–150 kHz disturbances increase losses in distribution lines and transformers, and can interfere with sensitive loads. Their findings align with the concerns raised by DAB deployments in fast-charging corridors, where supraharmonics propagate through medium- and low-voltage feeders.

Grid interaction studies are equally important. Grasel et al., analysed how V2G-enabled charging stations affect grid impedance up to 150 kHz, showing that active power electronic interfaces alter the network's frequency response, potentially magnifying interharmonics and resonances. This work is particularly relevant to bidirectional DAB converters, which inherently support V2G operation.

Transient effects have also received attention. Zhou and Tang proposed a Transient Current Balancing (TCB) modulation scheme for DAB converters under Triple Phase Shift (TPS) control. Their experimental results confirmed that during load steps, conventional TPS control introduces DC offsets and overshoot currents that excite interharmonic and supraharmonic frequencies. TCB modulation mitigates these transients, offering a pathway for grid-friendly DAB operation during dynamic charging events.

Converter design methodology has been revisited as well. García Pérez et al. classified dual active resonant bridge (resonant DAB) design approaches, detailing how leakage inductance, magnetizing inductance, and parasitic capacitances determine resonant behavior. These parameters not only affect efficiency but also shift the locations of resonant peaks, influencing both interharmonic and supraharmonic spectra. This reinforces the importance of incorporating non-ideal transformer models in grid impact studies.

Rajkumar et al. offered a comprehensive review on supraharmonics, framing them as the next major power quality challenge. Their synthesis of measurement techniques, propagation mechanisms, and mitigation strategies confirms that supraharmonics are underregulated yet increasingly significant in modern grids dominated by fast chargers and renewable converters.

Therefore, this paper explores the accurate estimation of interharmonic distortions caused by DAB converters in fast charging applications using sine wave correlation (SWC) method. This paper also suggests mitigation strategy by optimal selection of DAB parameters using Multi Sine Cosine Algorithm (MSCA).

2. INTERHARMONIC ESTIMATION USING SWC

In the proposed method, the estimates of frequencies and their corresponding magnitudes and phases are extracted using sine wave correlation (SWC). (Umadevi, A. et. al.,2022)

Any noise contaminated periodic signal can be organized in the following way:

$$u(t) = \sum_{n=1}^{N} A_n \sin(\omega_n t + \emptyset_n) + \gamma(t)$$
(1)

N is the number of harmonics in the system., $\omega_n = 2\pi f_0$, f_0 is the fundamental frequency and $\gamma(t)$ is the noise that is added to the signal. Accurate amplitude and phase estimation becomes more challenging in noisy environments. The influence noise in the estimation of signal can be largely reduced by using sine-fitting techniques.

The simpler form of sine-fitting that can be used to fit a wave is defined as:

$$u(t) = A_c \cos(2\pi f t) + A_s \sin(2\pi f t) + A_{DC}$$
(2)

where A_c and A_s are the in-quadrature sine amplitudes of the sine wave, f is the frequency of excitation and A_{DC} is the DC element.

If a single frequency signal is utilized for excitation, sine wave correlation (SWC) can be used to recover the signal amplitude from the obtained data set. Phase information may be retrieved using cosine and sine signal correlation. [Svilainis et al.]. Sine wave correlation is a general method for identifying the content of a sine wave in an input signal of a specific frequency and phase. This process is the foundation of the Fourier transform, and computing techniques established for general signal analysis can be used to discover the components of the signal produced when a sine wave is applied to system input.

The process for determining amplitude and phase can be simplified to make it more computationally efficient. The function equation (2) is fitted to the set of M samples, $u_1, u_2, ..., u_M$, attained at a frequency f_s at time intervals $t_1, t_2, ..., t_M$, is realized as:

$$A_C = \frac{\sum_{m=1}^{M} [\cos(2\pi f t_m).u_m]}{\sum_{m=1}^{M} [\cos(2\pi f t_m)]^2}$$
(3)

$$A_S = \frac{\sum_{m=1}^{M} [\sin(2\pi f t_m).u_m]}{\sum_{m=1}^{M} [\sin(2\pi f t_m)]^2}$$
(4)

$$A_{DC} = \frac{\sum_{m=1}^{M} u_m}{M} \tag{5}$$

Then the measured signal magnitude is given as

$$A = \sqrt{A_C^2 + A_S^2} \tag{6}$$

and the phase is given by

$$\emptyset = \arctan\left(\frac{A_S}{A_C}\right) \tag{7}$$

The SWC algorithm is first implemented for the extraction of frequencies and their corresponding magnitude and phases.

For the purpose of examining the interharmonics from DAB based EV fast charging system connected to grid, a Matlab Simulink model has been developed for a single-phase 10-kW DAB model consists of two MOSFET full-bridges linked by a coupling inductor and a high frequency transformer. The high voltage bridge is connected to the grid and universal bridge and the low voltage bridge is connected to a 450V DC source. Both bridges are controlled by a pulse generator and a current regulator. Figure 2 shows the Simulink model of the DAB connected grid used for this analysis.

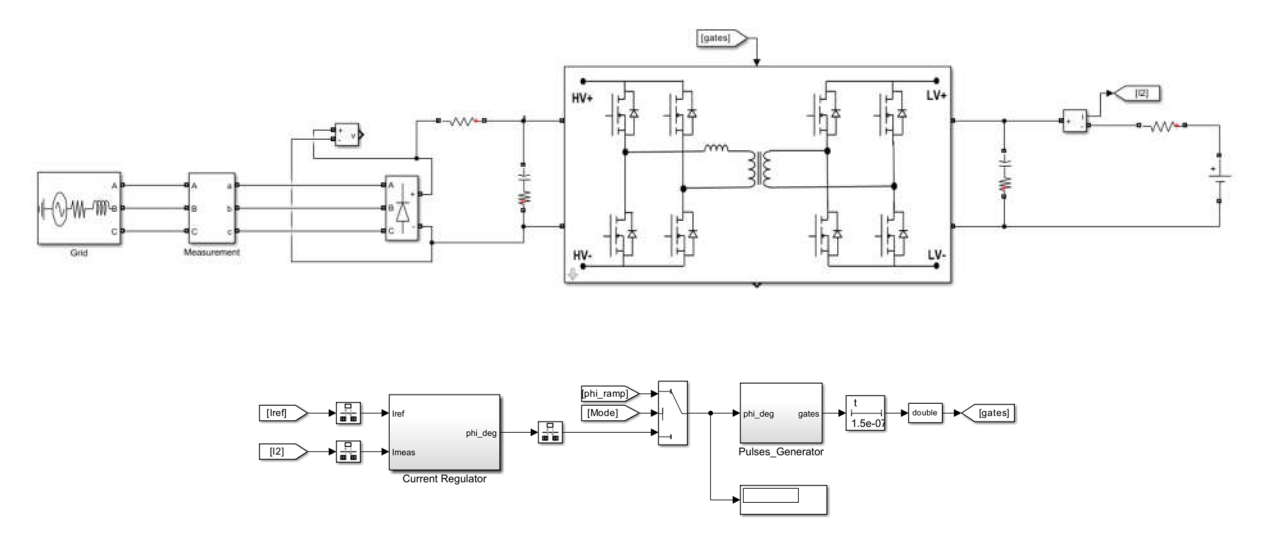


Fig. 2 Simulink model of the single-phase grid-connected DAB

Power flow in the DAB is achieved by phase-shifting the pulses of one bridge with respect to the other, while keeping the duty cycle of both bridges at 50%. Identical pulses are sent to the diagonal switches and the switching frequency is set to 100 kHz and the dead time to 150 ns. The theoretical output power transfer between the two bridges is given by:

$$P = \frac{V_{HV}NV_{LV}\phi(\pi - |\phi|)}{2\pi^2 F_{SW}L} \tag{8}$$

where V_{HV} is the DC link voltage of the high voltage bridge, in volts, N is the primary to secondary transformer voltage ratio, V_{LV} is the DC link voltage of the low voltage bridge, in volts, \emptyset is the phase shift between the two square waves of the bridges, in radians, F_{SW} is the PWM switching frequency, in hertz and L is the total inductance (coupling inductor + total transformer leakage reactance seen from the primary) between the two bridges, in henry. The proposed SWC methodology is employed for the estimation of interharmonics in the grid voltage.

3. OPTIMAL DESIGN OF DAB USING MULTI SINE COSINE ALGORITHM

Harmonic disturbances from DAB mainly arise from its phase-shift PWM switching and transformer behaviour. They manifest as low-order harmonics, high-frequency switching harmonics, and interharmonics. Proper filtering and modulation optimization are necessary to comply with grid power quality standards.

3.1 Selection of Variables of DAB

The design parameters of DAB are optimally selected using multi sine cosine algorithm MSCA in order to minimize the effect of interharmonics and harmonics in the grid.

3.1.1 Transformer Turns ratio

In a DAB with full bridges and an isolation transformer, power is transferred by phase-shifting the two square-wave bridge voltages by an angle Ø. The choice of transformer ratio N decides how close typical operating points are to the electrical balance, thereby setting the required phase shift, current stress, and soft-switching margins. The typical range of turns ratio varies between 1.6 and 2.2.

3.1.2 Phase Shift Modulation

Two full bridges produce 50% duty square waves of amplitudes V_{HV} (primary) and V_{LV}' (secondary reflected to the primary). The transformer's leakage inductance (plus any series inductor) is L referred to the same side. In phase-shift modulation the secondary bridge square wave is phase-shifted by an electrical angle $\emptyset \in (-\pi,\pi)$ with respect to the primary. If $\emptyset > \mathbf{0}$, power is transferred from HV side to LV side of DAB and if $\emptyset < \mathbf{0}$, the power transfer is reversed enabling V2G in EV charging.

3.1.3 Series Coupling Inductor

The series/leakage inductance in a DAB sets the power gain, shapes the current waveform, and provides the energy needed for ZVS commutations. Too large L risks loss of ZVS at light load and too small L inflates RMS/ripple and EMI. Therefore, L must be codesigned with turns ratio, switching frequency and \emptyset to meet efficiency, ZVS robustness, and ripple targets across the full voltage window. The typical range of turns ratio varies between 10 and $40\mu H$.

3.1.4 Switching Frequency

In a DAB, switching frequency F_{SW} scales the power transfer. higher the frequency lowers plant gain, allowing larger L and smaller \emptyset for the same power. Raising F_{SW} improves power density and can reduce RMS/ripple via larger L, but aggravates **core** and switching losses. Therefore, F_{SW} must be co-optimized with L and \emptyset to meet efficiency, thermal and ZVS robustness across the full voltage window. The typical range varies from 50 to 150kHz.

3.1.5 Gain Values of Current Regulator

The inner PI current regulator maps current error to phase shift. K_P sets bandwidth and disturbance rejection but is limited by delay-induced phase lag and noise. K_I removes steady-state error and shapes low-frequency behaviour but must be bounded to prevent wind-up and oscillation. Typical values of K_P varies in between 0.1 to 0.001 and K_I varies in between 10 to 300.

All the above variables have to be optimally selected to keep dynamics and margins consistent over the full EV charging range. Therefore, in this research Multi Sine Cosine algorithm (MSCA) has been employed for the optimal selection with the objective of minimizing the magnitudes of interharmonic components other than the fundamental component. (Umadevi, A. et. al.,2023)

3.2 Multi Sine Cosine Algorithm

Mirjalili (2016) invented the Sine-Cosine algorithm (SCA), a metaheuristic search method based on the sine and cosine functions in trigonometry. Using a mathematical model based on sine and cosine functions, the SCA generates numerous random solutions at first and encourages them to choose the best option. The sine or cosine function is given in Equation 9 or Equation 10 correspondingly, and the algorithm operates by looking for solutions in the search space.

$$Z_i^{t+1} = Z_i^t + x_1 \times \sin(x_2) \times |x_3 P_i^t - Z_i^t|$$
 (9)

$$Z_i^{t+1} = Z_i^t + x_1 \times \cos(x_2) \times |x_3 P_i^t - Z_i^t|$$
 (10)

where Z_i^t denotes the positions of the present i^{th} solution at t^{th} iteration. x_1 , x_2 and x_3 are the random variables. P_i is the destination solution and the symbol \parallel denotes the absolute value. The Equations (3.10) and (3.11) are unified into one function in Equation 11 as

$$Z_i^{t+1} = \begin{cases} Z_i^t + x_1 \times \sin(x_2) \times |x_3 P_i^t - Z_i^t| & \text{if } x_4 < 0.5\\ Z_i^t + x_1 \times \cos(x_2) \times |x_3 P_i^t - Z_i^t| & \text{if } x_4 \ge 0.5 \end{cases}$$
(11)

where x_4 is a number between 0 and 1 that is chosen at random. The parameter x_1 is a random number that determines the size of the area of the following solution, that could be either outside or inside the space between Z_i and P_i . The cyclic pattern of sine and cosine function allows a solution to be re-positioned around another solution. This can guarantee exploitation of the space defined between two solutions.

For exploring the search space, the solutions should be able to search outside the space between their corresponding destinations as well. To strike a balance between exploration and exploitation, the parameter, x_1 is adjusted using the equation below.

$$x_1 = d - t \frac{d}{T} \tag{12}$$

where, d is a constant, the total number of iterations is T, and the current iteration is t. The parameter x_3 is a random weightage for the target that is used to stochastically emphasize $(x_3 > 1)$ or deemphasize $(x_3 < 1)$ the target's significance in calculating the distance. The parameter, x_4 indicates equal switching between the sine and cosine parts, as seen in Equation (11). In 2021, Rehman et alsuggested MSCA (Multi Sine Cosine Algorithm) to avoid local optima convergence and promote exploitation. The MSCA algorithm enhances the SCA algorithm in two stages; the first stage offers a clustered population to diversify & intensify the search to avoid the local minima. Secondly, during the update, MSCA also checks for better clusters that offer convergence to global minima effectively. The proposed MSCA algorithm starts by generating random groupings of search agents i.e., $Z_1, Z_2, Z_3, ..., Z_n$ of equal sized population N, where each cluster $Z_i = [z_{i1}, z_{i2}, z_{i3}, ..., z_{in}]$ are initialized to provide a comprehensive solution to the specified problem. These clusters are then united to form a single group Z that provides a superior solution. The execution of MSCA is explained in the following algorithm.;

- 1. Random population groupings $Z_1, Z_2, Z_3, ..., Z_n$ are created at the start.
- 2. The value of x_1 is decreased from 2 to 0 over time.
- 3. If the value of $x_1>1$, more diversity is provided in the new single solution by merging all of the clusters using the greatest Euclidean distance as

$$Z_{1,n} = maxELD(Z_1, Z_2, Z_3, ..., Z_n)$$
 (13)

4. If the value of $x_1 < 1$, more diversity is provided in the new single solution by merging all of the clusters using the minimum Euclidean distance as

$$Z_{1,n} = minELD(Z_1, Z_2, Z_3, \dots, Z_n)$$

$$\tag{14}$$

- 5. The objective function f(Z) is used to evaluate each of the search agent clusters.
- 6. The best solution from all the clusters found so far is updated. (P = Z).
- 7. The random numbers x_1 , x_2 , x_3 and x_4 are updated.
- 8. Equations (13) and (14) are used to calculate the position of search agents.
- 9. The steps above are repeated until all of the conditions are satisfied or the iterations are completed.

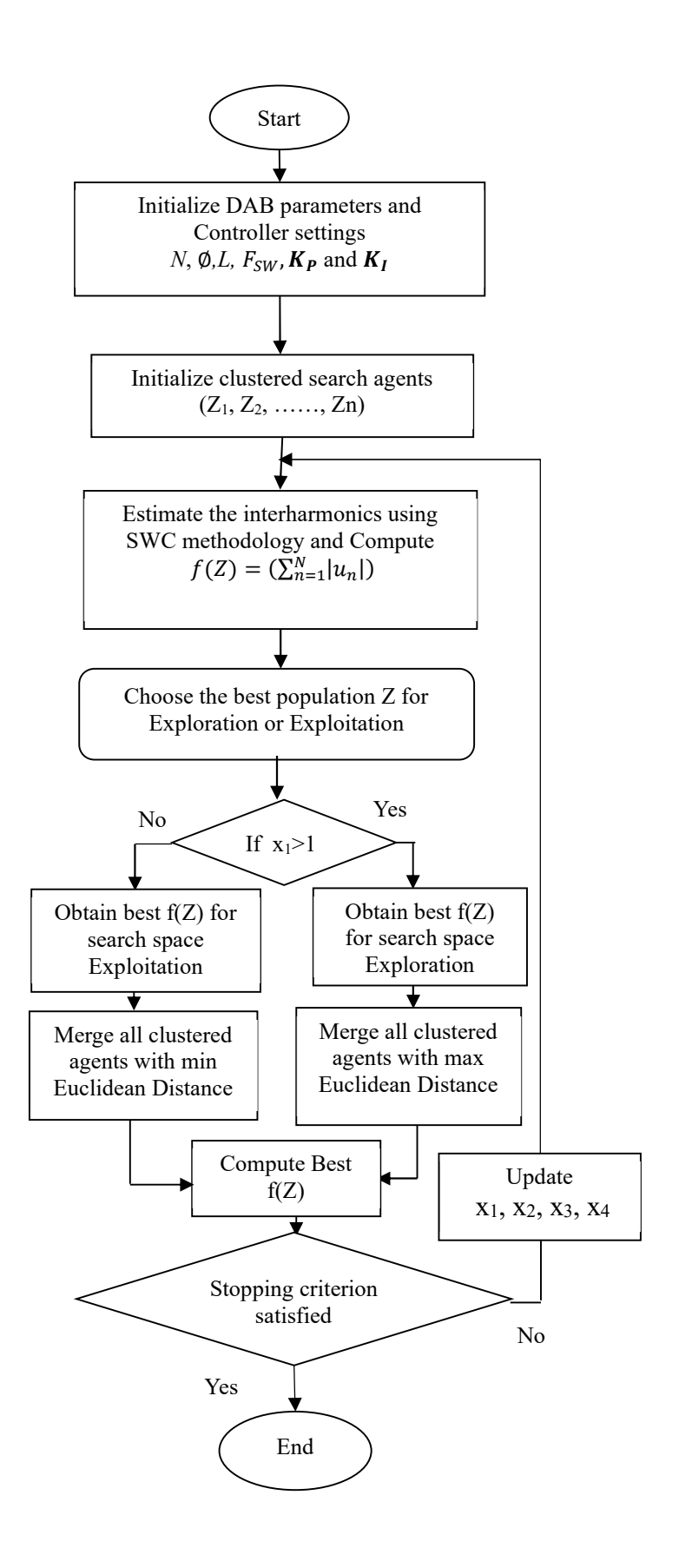


Fig. 4 Flow diagram of MSCA based DAB parameter selection for reduction of interharmonics

When compared with other evolutionary algorithms, the variables x_1 , x_2 , x_3 and x_4 that decide the convergence of algorithm are automatically adjusted and are independent of initial values. The purpose of this work is to reduce interharmonic components by optimal selection of DAB parameters and the gain values of current regulator using MSCA. Therefore, objective function for the MSCA optimization can be defined in terms of population Z as

$$minimize \ f(Z) = \sum_{n=1}^{N} |u_n| \tag{15}$$

where N represents the number of interharmonics components other than fundamental component. In the proposed MSCA based methodology, N, \emptyset , L, F_{SW} , K_P and K_I are chosen as variables for optimization. Figure 4 shows flow chart of the proposed MSCA based optimization methodology for determining the optimal DAB and controller for minimization of interharmonics.

4 Simulation Results

4.1 Estimation of interharmonics using SWC

For the purpose of estimation of interharmonics from DAB based EV fast charging system connected to grid, a Matlab Simulink model has been developed for a single-phase 10-kW DAB model consists of two MOSFET full-bridges linked by a coupling inductor and a high frequency transformer. The high voltage bridge is connected to the grid and universal bridge and the low voltage bridge is connected to a 450V DC source. Both bridges are controlled by a pulse generator and a current regulator. The control variables N, \emptyset , L, F_{SW} , K_P and K_I are chosen based on conventional design methodology. Figure 5 shows the presence of interharmonics around the fundamental frequency.

4.1 Optimal selection of DAB parameter using Hybrid SWC – MSCA methodology

For the same DAB system MSCA algorithm is employed for optimal selection of the control variables N, \emptyset , L, F_{SW} , K_P and K_I with the objective of minimizing the magnitude of interharmonics. The algorithm is run for 100 iterations and the best value is chosen. From Figure 5 it is observed that the magnitude of the interharmonics has significantly reduced.

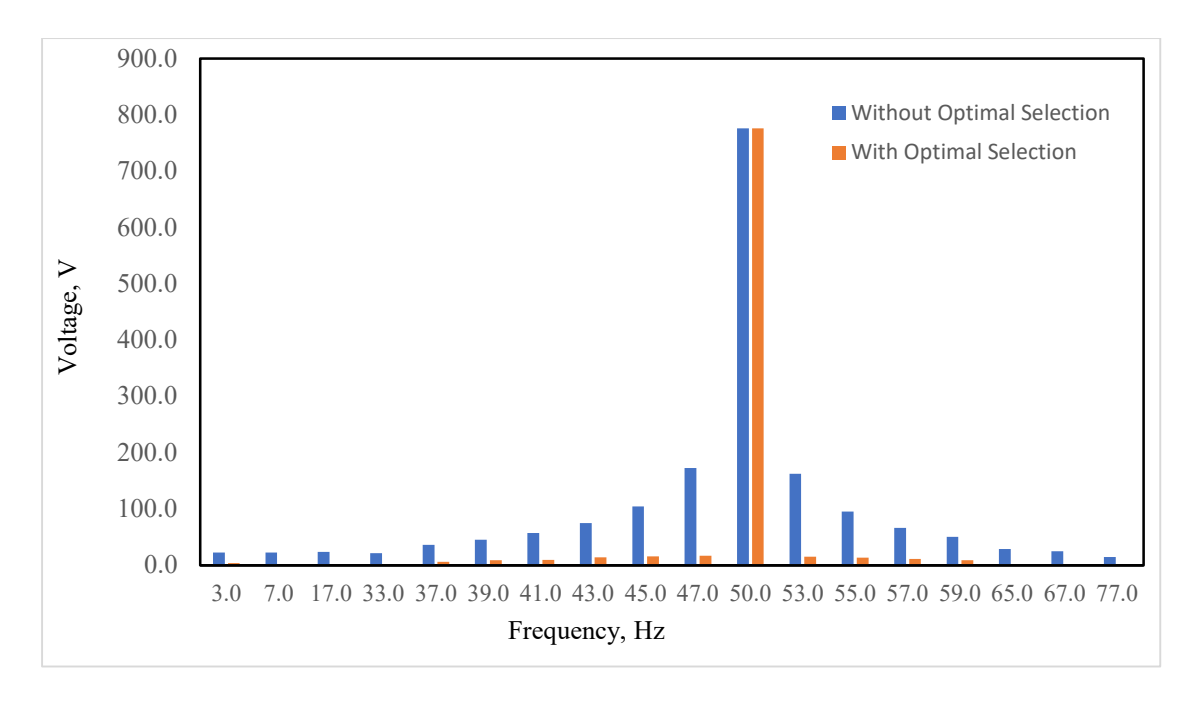


Fig. 5 Frequency spectrum of grid voltage with and without optimal selection of DAB parameters

It is observed that the transient nature of the current controller at the beginning are greatly minimized for the optimal parameter settings when compared with the normal DAB operation. Table 1 shows the comparison of the optimally selected parameters by the proposed hybrid SWC-MSCA based methodology and the conventional design values.

Table 1 Comparison of Optimal DAB Parameters and Controller Settings

DAB Parameters	Conventional Design Values	Optimal values using proposed methodology
N	1.6	1.8
Ø	-10	-10
L	15μΗ	45μΗ
F _{SW}	100kHz	130 kHz
K _P	0.1	0.5567
K _I	500	130.1263

5 Conclusion

In this paper DAB parameters and the gain values of current regulator are optimally tuned using the proposed hybrid SWC-MSCA based methodology to reduce the interharmonics created by the perturbation of the controller. The estimation of interharmonics emission is really important for the mitigation of interharmonics. The SWC- methodology is implemented for accurate estimation of interharmonics. Using the estimated values proposed algorithm finds optimal values for DAB parameters and controller settings. The suggested MSCA-based methodology's key advantage is that, unlike previous metaheuristic algorithms, it does not necessitate any effort in modifying algorithm-related parameters. This attribute distinguishes the suggested methodology as being advantageous in terms of ease of implementation.

References

- 1. **Ataullah, A., Rehman, A. U., Sher, H. A., and Khan, S. A.** "Analysis of the dual active bridge-based DC–DC converter topologies, high-frequency transformer and control techniques," *Energies*, vol. 15, no. 23, p. 8944, Dec. 2022. [Online].
- 2. Central Electricity Authority (CEA). Technical Standards for Connectivity of the Distributed Generation Resources. New Delhi, India: Ministry of Power, Govt. of India, 2019.
- 3. Cinik, Y., Zhao, X., and Bauer, P. "Efficiency and cost optimization for 350 kW DC fast chargers using modular DAB converters," *arXiv* preprint, Apr. 2024. [Online].
- 4. **European Commission JRC.** "Grid Harmonic Impact of Multiple Electric Vehicle Fast Charging," *Publications Office of EU*, 2018.
- 5. García Pérez, R. A., Azcondo, F. J., and Alou, P. "Classification of design methodologies of dual active resonant bridges," *Electronics*, vol. 13, no. 23, p. 4748, Dec. 2024. [Online].
- 6. Gill, L. Evaluation and Development of Medium-Voltage Converters: An MV Dual-Active-Bridge (DAB) Approach using 3.3 kV SiC MOSFETs for 800 V EV Fast Charging System, M.S. thesis, Virginia Tech, Blacksburg, VA, USA, 2019.
- 7. **Grasel, B., Roinila, A., and Jacobsen, M. Z.** "Impact of V2G charging stations (active power electronics) on the higher frequency grid impedance up to 150 kHz," *Sustainable Energy, Grids and Networks*, vol. 37, p. 101168, May 2024. [Online].
- 8. **IEC 61000-4-7.** *General Guide on Harmonics and Interharmonics Measurements and Instrumentation.* Geneva, Switzerland: IEC, 2019.
- 9. **IEEE Standard 519-2014.** Recommended Practice and Requirements for Harmonic Control in Electric Power Systems. Piscataway, NJ, USA: IEEE, 2014.
- 10. **Joarder, S., Forouzesh, M., and Khaligh, A.** "Harmonic modelling and control of dual active bridge," *Sustainable Energy, Grids and Networks*, vol. 40, p. 101251, Nov. 2024. [Online].
- 11. **Kumar, R., et al.** "Harmonic Amplification in EV Fast Charging Stations under Weak Grids," *Electric Power Systems Research*, 2021.

- 12. **Li, H., et al.** "High-Frequency Oscillation of the Active-Bridge-Transformer-Based DC/DC Converter," *Energies*, 2022.
- 13. Liang, X., Srdic, S., Won, J., Aponte, E., Booth, K., and Lukic, S. "A 12.47 kV medium-voltage input 350 kW EV fast charger using 10 kV SiC MOSFET," in *Proc. IEEE Applied Power Electronics Conf. and Exposition (APEC)*, Anaheim, CA, USA, Mar. 2019, pp. 581–587. doi: 10.1109/APEC.2019.8722239
- 14. **Mariscotti, A., Faifer, M., and Ferrero, A.** "The effects of supraharmonic distortion in MV and LV AC power networks," *Energies*, vol. 17, no. 3, p. 1105, Feb. 2024. [Online].
- 15. **Mirjalili, S.** "SCA: A Sine Cosine Algorithm for Solving Optimization Problems," *Knowledge Based Systems*, vol. 96, pp. 120–133, 2016.
- 16. **Mwasilu, F., et al.** "Power Quality Issues in Electric Vehicle Charging Infrastructure: A Review," *IEEE Trans. Industrial Electronics*, 2014.
- 17. **Padiyar, K. R. and Kulkarni, A. M.** "Analysis of Sub-Synchronous Resonance in Power Systems," *IEEE Trans. Power Delivery*, 2015.
- 18. Pan, Z., Wu, X., and Wang, H. "Second harmonic current reduction of dual active bridge under DPS from an impedance perspective," *Electric Power Systems Research*, vol. 237, p. 110374, Aug. 2024. [Online].
- 19. Qin, Z., van der Zee, S., Scott, M. J., and Bauer, P. "Modeling and control of dual active bridge converters under wide load range," *IEEE Trans. Power Electronics*, vol. 36, no. 7, pp. 7758–7772, Jul. 2021. [Online].
- 20. **Rahman, M., et al.** "Filter-Based Active Damping of DAB Converter to Lower Battery Degradation in EV Fast Charging Application," *IEEE/ResearchGate*, 2023.
- 21. **Rajkumar**, **S.**, **Balasubramanian**, **R.**, **and Kathirvelu**, **P.** "A comparative analysis of supraharmonic emission by DC fast chargers used for electric vehicle charging," *ResearchGate Preprint*, Jan. 2025. [Online].
- 22. Rajkumar, S., Balasubramanian, R., and Kathirvelu, P. "A comprehensive review on supraharmonics The next big power quality concern," *Smart Grid and Sustainable Energy*, vol. 9, no. 15, pp. 1–18, 2024. [Online].
- 23. **Rehman, M. Z., Khan, A., Ghazali, R., Aamir, M., and Nawi, N. M.** "A new Multi Sine-Cosine algorithm for unconstrained optimization problems," *Plos one*, vol. 16, no. 8, 2021. [Online].
- 24. **Svilainis**, **L. and Dumbrava**, **V.** "Amplitude and phase measurement in acquisition systems," *Matavimai*, vol. 2, no. 38, pp. 21–25, 2006.
- 25. **Umadevi, A. and Lakshminarasimman, L.** "Interharmonics estimation using hybrid multi sine cosine algorithm," *Int. J. Nonlinear Anal. Appl.*, vol. 13, no. 2, pp. 619–629, Jul. 2022, doi: 10.22075/ijnaa.2022.6453.
- 26. Umadevi, A., Lakshminarasimman, L., and Sakthivel, A. "Optimal design of shunt active power filter for mitigation of interharmonics in grid tied photovoltaic system," *Energy Reports*, vol. 9, pp. 3841–3853, Jun. 2023, doi: 10.1016/j.egyr.2023.05.066.
- 27. **Veerakgoundar, V. and Subramaniam, S. K.** "An efficient and compact voltage feed-forward DAB-based bidirectional DC–DC converter for onboard EV charger," *Comput. Electr. Eng.*, vol. 122, Mar. 2025, Art. no. 109979, doi: 10.1016/j.compeleceng.2024.109979.

- 28. **Xiong, W., et al.** "Supraharmonic Emission by DC Fast Chargers," *Nature Scientific Reports*, 2025.
- 29. **Zhou, S. and Tang, J.** "Transient current balancing modulation for seamless load step response in a DAB converter with triple phase-shift control," *Scientific Reports*, vol. 15, no. 4567, Feb. 2025. [Online].